Insulin-like Growth Factor-I Receptor Blockade Improves Outcome in Mouse Model of Lung Injury

Jung-Eun Choi[1]*, Sung-soon Lee[1]*, Donald A. Sunde[1], Isham Huizar[1], Kathy L. Haugk[2], Victor J. Thannickal[3], Ragini Vittal[3], Stephen R. Plymate[2], and Lynn M. Schnapp[1]

[1]Divison of Pulmonary and Critical Care Medicine, Department of Medicine, Harborview Medical Center, University of Washington, Seattle, Washington; [2]Department of Medicine, Harborview Medical Center, University of Washington, and Geriatrics Research Education and Clinical Center, Veterans Affairs Puget Sound Health Care System, Seattle, Washington; and [3]Divison of Pulmonary Medicine, Department of Medicine, University of Michigan Medical Center, Ann Arbor, Michigan

Rationale: **The insulin-like growth factor-I (IGF-I) pathway is an important determinant of survival and proliferation in many cells. However, little is known about the role of the IGF-I pathway in lung injury. We previously showed elevated levels of IGF-I in bronchoalveolar lavage fluid from patients with acute respiratory distress syndrome. Furthermore, immunodepletion of IGF from acute respiratory distress syndrome bronchoalveolar lavage increased fibroblast apoptosis.**

Objectives: **We examined the effect of blockade of type 1 IGF tyrosine kinase receptor (IGF-IR) in a murine model of bleomycin-induced lung injury and fibrosis.**

Methods: **Mice were treated with a monoclonal antibody against the IGF-I receptor (A12) or vehicle after intratracheal bleomycin instillation.**

Measurements and Main Results: **Mice treated with A12 antibody had significantly improved survival after bleomycin injury compared with control mice. Both groups of mice had a similar degree of fibrosis on days 7 and 14, but by Day 28 the A12-treated group had significantly less fibrosis. Delayed treatment with A12 also resulted in decreased fibrosis. A12-treated mice had significantly decreased apoptotic cells on Day 28 compared with control mice. We confirmed that A12 treatment induced mouse lung fibroblast apoptosis *in vitro*. In addition, IGF-I increased lung fibroblast migration. The primary pathway activated by IGF-I in lung fibroblasts was the insulin receptor substrate-2/phosphatidylinositol 3-kinase/Akt axis.**

Conclusions: **IGF-I regulated survival and migration of fibrogenic cells in the lung. Blockade of the IGF pathway increased fibroblast apoptosis and subsequent resolution of pulmonary fibrosis. Thus, IGF-IR may be a potential target for treatment of lung injury and fibrosis.**

Keywords: insulin-like growth factor; lung injury; lung fibrosis

Insulin-like growth factor-I (IGF-I) is an important factor involved in the development and normal homeostasis of many organs. IGF-I is also a potent survival factor, acting by inhibiting apoptosis and inducing proliferation in various cells (1, 2). Dysregulation of cell survival and proliferation is a feature of many lung diseases, including acute respiratory distress syndrome (ARDS) and idiopathic pulmonary fibrosis. However, little is known about the role of the IGF pathway in these lung diseases. In the lung, IGF-I was originally described as alveolar macrophage–derived growth factor (3). IGF-I mRNA is elevated in bleomycin-induced pulmonary fibrosis in mice (4) and increased IGF-I immunostaining is observed on lung biopsies from patients with fibroproliferative ARDS (5).

We demonstrated that IGF-I is elevated in bronchoalveolar lavage fluid (BALF) from patients with early ARDS (6). We also showed that IGF-I in ARDS BALF provided a prosurvival signal for lung fibroblasts, but not lung epithelial cells (6). One of the interesting features about ARDS is that the lung injury resolves in the vast majority of patients. Apoptosis of lung fibroblasts may be an essential part of this resolution and the decrease in IGF-I levels may be an important permissive activity for the apoptosis of fibroblasts to occur (7–9).

To determine the role of IGF in the pathogenesis of lung injury, we analyzed the effect of blockade of IGF signaling through the IGF-I receptor (IGF-IR) in a murine model of bleomycin-induced lung injury and fibrosis.

AT A GLANCE COMMENTARY

Scientific Knowledge on the Subject

Insulin-like growth factor (IGF) levels have been shown to be elevated in early acute respiratory disease syndrome (ARDS) and decreased in late ARDS. However, it is unknown if decreased IGF contributed to the resolution of ARDS.

What This Study Adds to the Field

We found that an antibody against IGF-I receptor (IGF-IR) improved survival and resolution of fibrosis in bleomycin-treated mice. Thus, IGF-IR is a potential target for treatment of lung injury and fibrosis.

METHODS

Cells and Reagents

We isolated lung fibroblasts from C57BL/6 mice as previously described (10). Cells were maintained in Dulbecco's modified Eagle's medium−10% fetal bovine serum (FBS), penicillin (100 IU/ml)–streptomycin (100 μg/ml), and 2 mM L-glutamate. All cells were used by passage 6. Function-blocking antibody to the human type I IGF receptor (A12) was a generous gift from D. Ludwig (ImClone Systems, New York, NY) (11, 12). A12 inhibits IGF-IR signaling in murine and human tissues and does not cross-react with the insulin receptor (IR) (11). We verified that our preparation of A12 was endotoxin free by *Limulus* amebocyte lysate assay (Cambrex Bio-Science, Walkersville, MD).

Antibodies to insulin receptor substrate (IRS)-1, IRS-2, extracellular signal–regulated kinase (ERK), and phosphorylated ERK (pERK) were purchased from Santa Cruz Biotechnology (Santa Cruz, CA);

(*Received in original form February 6, 2008; accepted in final form November 11, 2008*)

Supported by an AHA grant-in-aid and by National Institutes of Health grants R01 HL73028, HL083481, SCCOR P50 HL073996, and R01-HL077555 (L.M.S.), and by Veterans Affairs Research Service and U54 CA 126540 (S.R.P.).

* J.-E.C. and S.-s.L. contributed equally to this work.

Correspondence and requests for reprints should be addressed to Lynn M. Schnapp, M.D., Box 358052, 815 Mercer Street, Seattle, WA 98109. E-mail: lschnapp@u.washington.edu

Am J Respir Crit Care Med Vol 179. pp 212–219, 2009
Originally Published in Press as DOI: 10.1164/rccm.200802-228OC on November 14, 2008
Internet address: www.atsjournals.org

antibodies to phospho-IRS-1 (pSer-312) and phospho-IRS-2 (pSer-731) were purchased from AnaSpec, Inc. (San Jose, CA); antibodies to Akt and pAkt (pSer-472/473/474) were purchased from BD Biosciences (San Jose, CA); horseradish peroxidase–conjugated anti-rabbit antibodies were purchased from Rockland (Gilbertsville, PA); and horseradish peroxidase–conjugated anti-mouse antibodies were purchased from Zymed (San Francisco, CA). IGF-I was purchased from R&D Systems (Minneapolis, MN).

Bleomycin-induced Lung Injury

All animal experiments were approved by the Institutional Animal Care and Use Committee of the University of Washington (Seattle, WA). C57BL/6 male mice underwent intratracheal instillation with 0.075 U of bleomycin (SICOR Pharmaceuticals, Inc., Irvine, CA) as previously described (13). A blocking antibody to IGF-IR, A12 (40 mg/kg) (12), or an anti–keyhole limpet hemocyanin isotype control antibody was injected intraperitoneally at the time of initial bleomycin instillation and two times per week for the duration of the experiment. Mice were killed at baseline (day 0, n = 3) or at 7 days (n = 12), 14 days (n = 18), or 28 days (n = 12) after initial bleomycin instillation, or earlier if they met predetermined criteria for euthanasia (14). In some experiments, A12 or control antibody administration was begun on Day 7 after bleomycin instillation and continued two times per week for an additional 14 days. At the time of death, the right main stem bronchus was tied off and the left lung was isolated and lavaged with 1 ml of phosphate-buffered saline (PBS) containing 0.6 mM ethylenediaminetetraacetic acid (EDTA) warmed to 37°C. BALF total cell count was determined by trypan blue exclusion and cell differential was determined on Diff-Quik (Dade Behring AG, Düdingen, Switzerland)–stained cytospins. After brief centrifugation, cell-free supernatants were used for measurement of total protein by Bio-Rad protein assay (Bio-Rad Laboratories, Hercules, CA). The left lung was snap frozen and used for hydroxyproline measurement as previously described (15). Hydroxyproline concentration was extrapolated from a standard curve. The right lung was inflated at a pressure of 25 cm H_2O and fixed with 4% paraformaldehyde for histologic evaluation.

Immunohistochemistry

Sections obtained from paraffin-embedded, fixed lungs underwent antigen retrieval by boiling sections in 10 mM sodium citrate buffer (pH 6.0). Endogenous peroxidase activity was quenched by incubation in 1% H_2O_2 for 10 minutes. To block nonspecific binding of immunoglobulins, slides were incubated with 1.5% goat serum in PBS for 1 hour at room temperature. Sections were incubated with IGF-IR-α antibody (diluted 1:200; Santa Cruz Biotechnology) overnight at 4°C and then incubated with biotinylated goat anti-rabbit antibody (diluted 1:200; Santa Cruz Biotechnology) for 30 minutes at room temperature. Sections were processed with VECTASTAIN ABC kit (Vector Laboratories, Burlingame, CA) followed by staining with 3,3′-diaminobenzidine (DAB peroxidase kit; Vector Laboratories) according to the manufacturer's instructions. Slides were then counterstained with hematoxylin, dehydrated, and mounted with permanent aqueous medium (Permount; Thermo Fisher Scientific, Waltham, MA).

To quantitate fibrosis, two independent blinded observers scored each animal on the basis of a previously developed scoring system (16) and the average score was used. Briefly, the right middle lobe was sectioned along the long axis, stained with hematoxylin and eosin, and systematically scanned with a microscope, using a ×10 objective. Each successive field was assessed for severity of fibrosis and given a score between 0 and 8 (0, normal lung; 8, total fibrous obliteration of the field) (16). In each field, the predominant degree of fibrosis was scored, that is, that which occupied more than half of the field area. After examining the whole section, the mean score of all the fields was used as the observer's fibrosis score.

For the terminal deoxynucleotidyltransferase dUTP nick end labeling (TUNEL) assay, tissue sections were deparaffinized by standard protocols and permeabilized with proteinase K (10 μg/ml in 10 mM Tris-HCl) for 30 minutes at 37°C. Nonspecific binding sites were blocked with bovine serum albumin (1 mg/ml) in 50 mM Tris-HCl for 10 minutes at 37°C. TUNEL-positive cells were detected with *In Situ* Cell Death Detection Kit, Fluorescein (Roche, Indianapolis, IN). Nuclei were counterstained with 4′,6-diamidino-2-phenylindole dihydrochloride (DAPI; Roche). To quantitate apoptosis, at least two mice per time point were examined and a blinded observer counted the number of TUNEL-positive cells and DAPI-positive cells in four independent fields per mouse. At least 500 cells were analyzed per condition.

Real-time Polymerase Chain Reaction

Total RNA was isolated from lungs on Days 0, 1, 3, 7, 14, 21, and 28 after bleomycin treatment, using an RNeasy Midi Kit (Qiagen, Valencia, CA) as per the manufacturer's specifications. Total RNA was reverse transcribed to cDNA with High-capacity cDNA Archive Kit (Applied Biosystems, Foster City, CA). Real-time polymerase chain reaction (PCR) was done with an ABI 7900HT system (Applied Biosystems) with the use of predesigned primers and probes (ABI TaqMan gene expression assays) for hypoxanthine–guanine phosphoribosyltransferase (HPRT) (as endogenous control) and IGF (as target probe). Analysis was done with Excel (Microsoft, Redmond, WA), calculating relative quantity (RQ) by the δ–δ cycle threshold (2-ddCt) method. At least five mice per time point were examined. *P* values were calculated using the Bonferroni correction for multiple comparisons.

Proliferation and Apoptosis Assays

For the proliferation assay, primary mouse lung fibroblasts were plated at 10,000 cells per 100 μl in 96-well plates. After initial adhesion, medium was changed to serum-free medium for overnight incubation and then IGF-I (100 ng/ml) was added. As a positive control, cells were grown in 10% FBS; as a negative control, cell were grown in serum-free medium. Cell proliferation was assayed at 48, 72, or 96 hours by cell proliferation kit (MTT; Roche) assay according to the manufacturer's directions. The optical density of plates was determined with a microplate reader (SpectraMax 250; Molecular Device, Sunnyvale, CA) at 570 nm. All experiments were done in triplicate and repeated three times.

For the apoptosis assay, primary mouse lung fibroblasts were plated in 96-well plates (20,000 cells per well) overnight and serum starved for 24 hours. Functional blocking antibody to the type I IGF receptor (A12) was added to medium at the indicated concentration for 24 hours. At the end of the experiment, plates were centrifuged at 200 × *g* for 10 minutes to prevent detached cells from being aspirated, and apoptosis was measured with the Cell Death Detection ELISA^{PLUS} system (Roche), which detects cytosolic histone–complexed DNA fragments. All experiments were done in triplicate and repeated at least twice. The apoptosis index was defined as the ratio of the optical density at 405 nm ($OD_{405\ nm}$) of the experimental condition to that of the control (medium alone) condition.

Migration Assay

Primary mouse lung fibroblasts (50,000 cells per well) were plated in serum-free medium overnight on FluoroBlok transwell filters (BD Falcon HTS FluoroBlok 24-multiwell insert system, 8-μm pores; BD Biosciences) precoated with fibronectin (50 μg/ml). FluoroBlok microporous membranes are specifically designed to detect by fluorescence only cells below the surface membrane. IGF-I (100 ng/ml), 10% FBS (positive control), or serum-free medium (negative control) was added to the lower chamber. In some experiments, cells were preincubated with the blocking antibody to IGF-IR (A12, 40 μg/ml) for 1 hour. After 4 hours of migration, filters were fixed with formaldehyde and stained with DAPI. Migrated cells were counted in three predesignated fields for each filter. All experiments were done in triplicate and repeated at least three times.

Western Blot Analysis

Cells were grown to 70% confluence and placed in serum-free medium overnight, and then IGF-I (100 ng/ml) was added for 5, 10, 15, 30, and 60 minutes. At the indicated time points, cells were washed in ice-cold PBS and lysed in buffer containing 100 mM Tris-HCl (pH 7.4), 150 mM NaCl, 1 mM $CaCl_2$, 0.1% sodium dodecyl sulfate, 1% Triton-X, 0.1% Nonidet P-40, 1 mM $NaVa_3$ (sodium vanadate), 1 mM NaF (sodium fluoride), and protease inhibitor cocktail tablet (Roche). Protein concentrations were determined by the bicinchoninic acid assay (Pierce Biotechnology, Rockford, IL). Equal amounts of protein were sepa-

rated by sodium dodecyl sulfate–polyacrylamide gel electrophoresis, and electrophoretically transferred to polyvinylidene difluoride membrane. Membranes were blocked with 5% nonfat dry milk−0.05% Tween 20–PBS for 2 hours, incubated with primary antibody for 2 hours at room temperature, washed with 0.05% Tween 20–PBS, incubated with horseradish peroxidase–conjugated secondary antibody (diluted 1:5,000) for 1 hour, washed with 0.05% Tween 20–PBS, and then developed by the enhanced chemiluminescence technique (Amersham, Little Chalfont, UK).

Statistical Analysis

Means of more than two groups of data were compared by one-way analysis of variance (ANOVA) for analysis of one independent variable or by two-way ANOVA, for analysis of two independent variables, followed by Tukey's honestly significant difference post-hoc test. The Student *t* test was used for comparison of paired parametric data. All tests were two tailed and *P* values not exceeding 0.05 were considered significant. Kaplan-Meier survival analysis was performed with JMP-IN version 5.1 (SAS Institute, Cary, NC); statistical significance was determined by log-rank test.

RESULTS

Time Course of IGF Expression after Bleomycin Injury

We previously demonstrated in patients that IGF was up-regulated early in ARDS, and decreased in late ARDS (6). We analyzed IGF expression after bleomycin injury in mice by quantitative real-time PCR and found significantly increased IGF mRNA expression by Day 1 after bleomycin administration; expression peaked on Day 7 (7-fold increase) (Figure 1). IGF mRNA levels decreased at later time points, but remained elevated on Day 14 compared with baseline levels.

Down-regulation of IGF-IR in A12-treated Mice

A12 inhibits IGF-I signaling by two mechanisms: (*1*) blockade of ligand binding to IGF-IR and (*2*) rapid induction of internalization and degradation of IGF-IR (11). Therefore, to verify the efficacy of A12 treatment, we examined IGF-IR expression in the lungs of A12 mice and control mice on Day 7 after bleomycin treatment. We found a marked decrease in IGF-IR expression in A12-treated mice, demonstrating the predicted effect of antibody administration in lung tissue (Figure 2).

Improved Survival of A12-treated Mice after Bleomycin Instillation

We tested the effect of a blocking antibody to IGF-I receptor, A12, in the bleomycin injury model. After bleomycin treatment, A12-treated mice (n = 24) showed a statistically significant survival benefit compared with control mice (n = 18, $P = 0.03$) (Figure 3). In the control group, most deaths occurred between 7 and 10 days, as expected in this model. Of note, A12 treatment of bleomycin-exposed mice resulted in significantly greater weight loss compared with control mice (20 vs. 13% by Day 14), but the mice had less evidence of respiratory or systemic distress as measured by body condition scoring (14). In the absence of bleomycin, administration of A12 alone had no effect on survival, lung histology, BALF protein concentration, or cell count (data not shown).

No Difference in Cell Count and Total Protein Concentration in BALF

To assess whole lung permeability and degree of inflammation, we measured total protein, cell count, and cell differentials in BALF. As expected, bleomycin-treated mice had significantly elevated total protein and cell count compared with untreated (Day 0) mice. At the early time points (Days 7 and 14) there

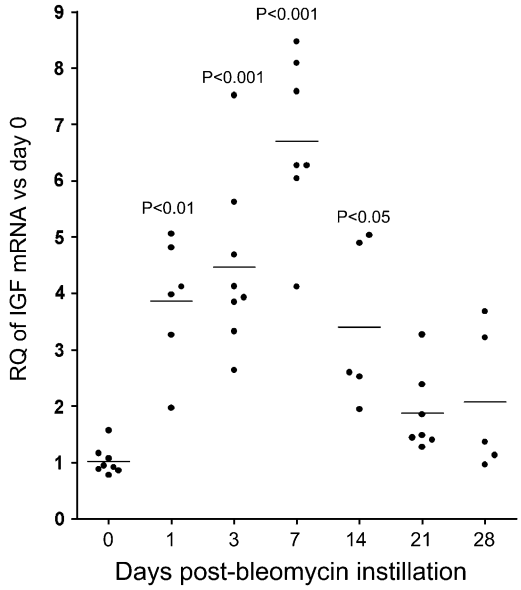

Figure 1. Real-time polymerase chain reaction analysis of insulin-like growth factor (IGF) mRNA expression after bleomycin administration. Data are normalized to hypoxanthine–guanine phosphoribosyltransferase expression. The *y* axis represents fold increase compared with Day 0. Each point represents an individual mouse. Mean values are indicated. RQ = relative quantity.

was no difference in BALF protein concentration in bleomycin–A12 versus bleomycin–control mice. By 28 days, there was a decreased BALF protein concentration in A12-treated mice compared with control mice (Figure 4A).

Although the total cell counts were not significantly different between A12 and control mice, there was a trend toward decreased cells in A12-treated mice (Figure 4B). There was no difference in cell differential between the two groups at any of the time points tested.

Lung Fibrosis

We measured hydroxyproline content of lungs as a marker of lung fibrosis. There were no significant differences in hydrox-

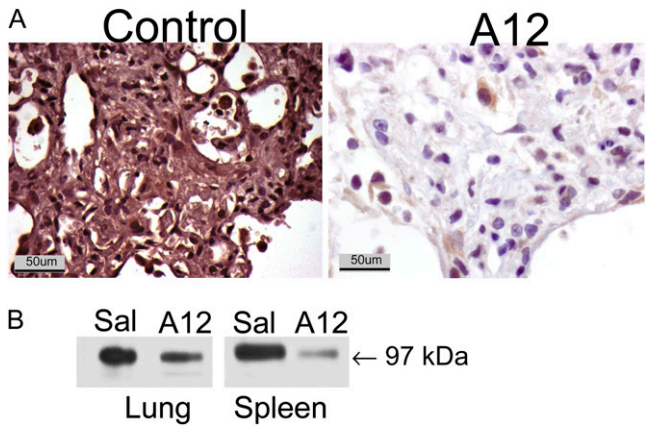

Figure 2. Decreased insulin-like growth factor-I receptor (IGF-IR) expression after systemic administration of A12, a monoclonal antibody against IGF-IR. (*A*) Immunohistochemical analysis for IGF-IR was performed on lungs on Day 7 after bleomycin administration. (*B*) Western blot analysis for IGF-IR, performed on lung and spleen lysates on Day 14 after bleomycin administration to mice treated with saline (Sal) or A12.

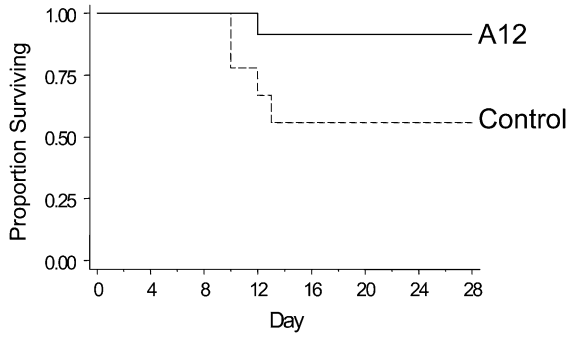

Figure 3. Kaplan-Meier survival curves for control and A12-treated mice after bleomycin treatment. The difference in survival was significant: $P = 0.038$, A12 versus saline (control).

yproline content on Days 7 and 14 between the two groups (Figure 5). However, on Day 28, there was significantly less hydroxyproline in A12-treated mice compared with control ($P = 0.03$) or compared with Day 14 measurements ($P = 0.001$), suggesting A12 treatment affected resolution of fibrosis rather than initial establishment of fibrosis.

Histology and fibrosis scores confirmed the hydroxyproline measurements (Figure 5). In all mice, right middle lobe histology is shown, because we were able to visualize the majority of the lobe under low magnification to allow for global assessment of injury and to minimize bias due to the patchy nature of bleomycin injury. At 14 days both groups showed areas of fibrosis, although there seemed to be qualitatively less fibrosis in A12-treated mice (Figures 5A–5H). However, the difference was more pronounced by Day 28 (Figures 5I–5P). On Day 28 after bleomycin instillation, the right middle lobes from control mice were smaller, had more distortion of normal lung architecture, and more areas of airspace obliteration and interstitial thickening, whereas right middle lobes from A12-treated mice had better preservation of lung architecture and lung size, and fewer areas of fibrosis.

To determine whether A12 administration was effective after initiation of injury, we delayed administration of A12 until 7 days after initial bleomycin injury and then analyzed fibrosis on Day 21 after initial injury. We found that there was decreased hydroxyproline, suggesting that A12 administration is also effective at decreasing fibrosis after initiation of the inflammatory process. Similar to previous findings, there was no difference in BALF total protein or cell count (Figure 6).

Apoptosis in Lungs of Bleomycin-treated Mice

To examine a potential mechanism of decreased hydroxyproline content, we compared the number of apoptotic cells in A12- and vehicle-treated mice. At the early time point (Day 14), there was a trend toward increase in TUNEL-positive cells in A12-treated mice (Figure 7), although this did not achieve statistical significance. On Day 28, there were significantly fewer apoptotic cells in A12-treated mice compared with vehicle-treated mice ($P < 0.05$).

Blockade of IGF-I Receptor Induced Apoptosis of Fibroblasts

We previously showed that blockade of the IGF pathway in human lung fibroblasts increased apoptosis under conditions of serum starvation (6). We have now expanded our initial findings and show that blockade of the IGF pathway with A12 antibody similarly induced a dose-dependent increase in apoptosis of primary mouse lung fibroblasts (Figure 7C). Thus, *in vivo* and *in vitro* data demonstrate that A12 treatment increases fibroblast apoptosis.

IGF-I Does Not Increase Proliferation of Mouse Lung Fibroblasts

Previous work demonstrated that IGF-I induced proliferation in several different cell types including pleural mesothelial cells (18), myeloma cells (17), and myoblasts (19). Because fibroblast proliferation is a key feature of pulmonary fibrosis (20), we asked whether IGF-I was mitogenic for normal lung fibroblasts. We compared cell proliferation in the presence or absence of IGF-I (100 ng/ml) for 24, 48, 72, and 96 hours, under serum-free conditions. In contrast to other reports, we did not see increased proliferation at any of the time points tested (Figure 8). Thus, the prosurvival benefit of IGF in fibroblasts appears to be due to an antiapoptotic, rather than proproliferative, signal.

IGF-I Induced Migration of Mouse Lung Fibroblasts

Migration of fibroblasts into intraalveolar spaces with subsequent deposition of extracellular matrix proteins is seen in pulmonary fibrosis. We previously found increased IGF in the BALF of patients with acute lung injury (6). Therefore, we asked whether IGF could act as a chemotactic factor for fibroblasts. We examined the migration of mouse lung fibroblasts in response to IGF, using a transwell filter system. We found that IGF-I increased migration of mouse lung fibroblasts compared with serum-containing medium (Figure 9). Treatment with blocking antibody to IGF-IR (A12) abrogated the increased migration.

IGF Signaling Pathways in Lung Fibroblasts

To determine the signaling pathways activated by IGF in lung fibroblasts, we first examined the expression and phosphorylation of IGF-IR after stimulation with IGF (Figure 10A). IGF-IR was phosphorylated within 15 minutes of IGF stimulation. We then examined lung fibroblasts for the presence of the major IRS, IRS-1, and IRS-2, and examined their phosphorylation after IGF stimulation (Figure 10B). We found that although fibroblasts express both IRS-1 and IRS-2, only IRS-2 was activated after IGF stimulation (Figure 10B). IRS-1 showed a constitutive level of phosphorylation that did not change after stimulation with IGF. IRS-2, on the other hand, showed in-

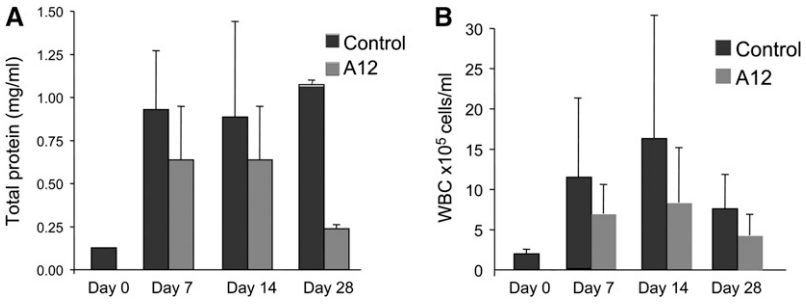

Figure 4. Bronchoalveolar lavage fluid (BALF) total protein concentrations (*A*) and cell count (*B*) at 0 (baseline), 7, 14, and 28 days after bleomycin instillation in A12-treated mice and control mice. Average values and SD are shown. WBC = white blood cells.

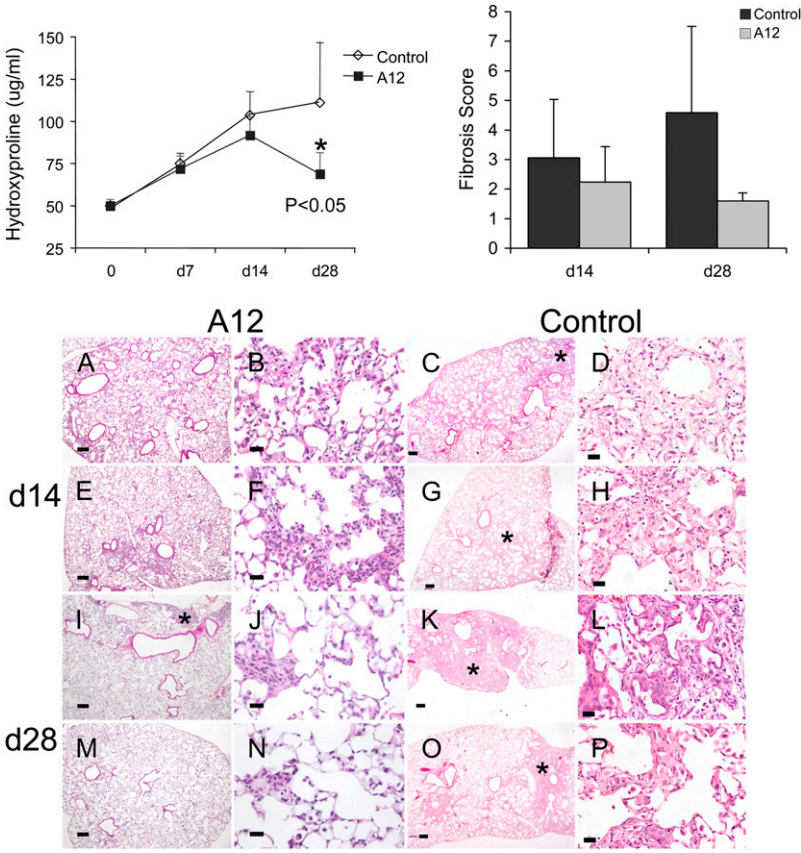

Figure 5. *Top*: Hydroxyproline content (*left*) and fibrosis scores (*right*) from A12-treated mice and control mice after bleomycin instillation. Data were analyzed by two-way analysis of variance (ANOVA) with Tukey's honestly significant difference (HSD) post-hoc test, and statistical significance was set at $*P < 0.05$. *Bottom*: Histology of A12-treated mice and control mice at 14 days (*A–H*) and 28 days (*I–P*) after bleomycin instillation. Lung sections from A12-treated mice show relatively normal interstitium and less fibrosis (*) compared with control mice. Right middle lobe samples from two mice per group are shown. Original magnification: (*A*, *C*, *E*, *G*, *I*, *K*, *M*, and *O*) ×4; (*B*, *D*, *F*, *H*, *J*, *L*, *N*, and *P*) ×40. *Scale bars*: (*A*, *C*, *E*, *G*, *I*, *K*, *M*, and *O*) 200 μm; (*B*, *D*, *F*, *H*, *J*, *L*, *N*, and *P*) 25 μm. Stained with hematoxylin and eosin.

creased phosphorylation by 5–10 minutes that decreased to baseline levels again by 30 minutes. Both phosphatidylinositol 3-kinase (PI3 kinase) and mitogen-activated protein kinase (MAPK) pathways have been implicated in IGF signaling in various cell types. We found that Akt, the downstream substrate of PI3 kinase, was phosphorylated in response to IGF-I stimulation by 15 minutes and persisted until 60 minutes (Figure 10C). In contrast, ERK, the downstream substrate of MAPK/ERK kinase (MEK)-1/2, is present in lung fibroblasts but did not undergo phosphorylation after stimulation with IGF-I (Figure 10C). Thus, in primary mouse lung fibroblasts, it appears that IRS-2 and PI3 kinase are the major pathways activated by IGF-I under the conditions tested.

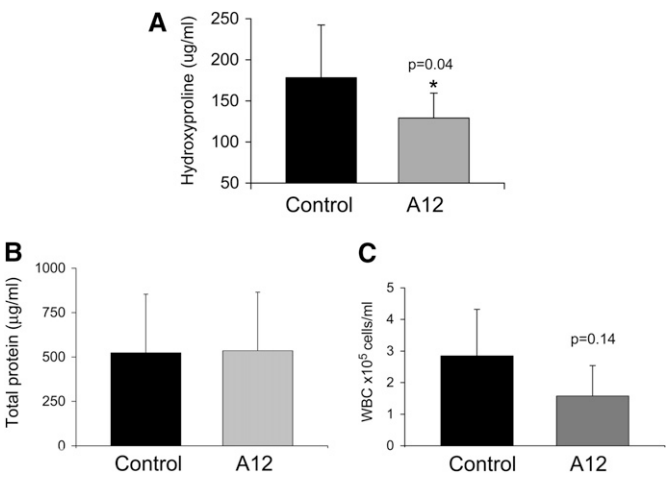

Figure 6. Hydroxyproline content (*A*), bronchoalveolar lavage fluid (BALF) total protein (*B*), and BALF total cell count (C) on Day 21 after bleomycin instillation and initiation of A12 antibody administration on Day 7. n = at least five animals per group. Average values and SD are shown.

DISCUSSION

We found that initial treatment with A12 antibody improved survival and hastened resolution of fibrosis after bleomycin-induced lung injury. Whereas initial fibrosis was similar in A12 and control mice, there was a significant decrease in hydroxyproline content in A12-treated mice from Day 14 to Day 28. We found that late administration of A12 was also effective at decreasing fibrosis. We also demonstrated that A12 treatment induced apoptosis in mouse lung fibroblasts *in vitro*. An unanswered and important question in pulmonary fibrosis concerns whether matrix remodeling can be affected after pulmonary fibrosis has occurred. It has been proposed that apoptosis of fibrogenic cells (i.e., fibroblasts) is essential for the resolution of lung injury (7, 9, 21). Because the IGF pathway is a key determinant of cell survival, down-regulation of this pathway may be necessary both for normal scarring to resolve and to prevent a prolonged fibrogenic response (i.e., fibrosis). Because the increased apoptosis preceded the improvement in fibrosis on Day 28, we speculate that this caused the improved fibrosis by eliminating the fibrogenic cells (8).

IGF regulates a number of functions that are relevant to the development of fibrosis including proliferation, collagen synthesis, and cell survival (22, 23). However, the contribution of IGF in animal models of fibrosis has been mixed. In a model of chronic renal failure due to subtotal nephrectomy, blockade of IGF resulted in less compensatory kidney growth, but no difference in renal function or fibrosis (24). Transgenic mice

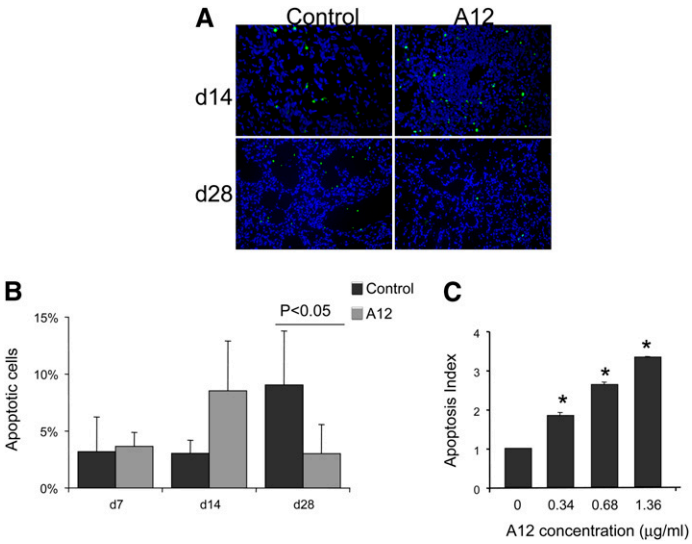

Figure 7. (*A*) Terminal deoxynucleotidyltransferase dUTP nick end labeling (TUNEL)-positive cells (*green*) in saline- and A12-treated mouse lungs on Days 14 and 28 after bleomycin injury. Nuclei are counterstained with 4′,6-diamidino-2-phenylindole (DAPI). Original magnification: ×20. (*B*) Quantification of TUNEL IHC by determining the number of TUNEL-positive cells per total number of cells. Shown is the average and SD of two mice per condition, with at least 500 cells analyzed per condition. Data were analyzed by two-way analysis of variance with Tukey's honestly significant difference (HSD) post-hoc test. (*C*) Increased apoptosis of primary mouse lung fibroblasts treated with insulin-like growth factor-I receptor (IGF-IR) antibody. Mouse lung fibroblasts were serum starved overnight and then incubated with the indicated concentration of IGF-IR antibody A12. Apoptosis was measured with Cell Death Detection ELISA^{PLUS} (Roche Applied Science). All experiments were done in triplicate and repeated at least twice. The apoptosis index is defined as follows: the ratio of the optical density at 405 nm ($OD_{405\ nm}$) of the experimental condition to that of the control condition (medium alone). *$P < 0.05$ compared with the control group.

expressing the IGF-IA splice variant under the control of the surfactant protein C promoter in the lung developed adenomatous hyperplasia, but not fibrosis (25). As noted by the authors, lack of fibrosis in their transgenic model may be due to secretion of IGF-IA into the lumenal compartment, rather than the interstitial compartment; lack of overexpression of IGF-IB splice variant; or decreased bioavailability of IGF by binding to insulin growth factor–like binding proteins.

IGF-I was implicated as a fibroblast mitogen in BALF from patients with sarcoidosis (26) and systemic sclerosis (27). IGF did not contribute to fibroblast proliferation in BALF from patients with asbestosis (28). In our experiments, IGF-I mediated cell survival and migration, but not proliferation, of normal lung fibroblasts through IGF-IR. The prior studies used either the fetal fibroblast cell line IMR-90 or human fetal embryonic fibroblasts (HFL-1) to examine the proliferative response (26, 27). In contrast, we used early-passage primary adult lung fibroblasts, which may account for the differences in results. In addition, the mitogenic response to IGF in the earlier studies was determined by immunodepletion of IGF from BALF (26, 27). We speculate that activation of fibroblasts by other growth factors or cytokines such as transforming growth factor-β_1 in BALF is necessary for the proproliferative effect of IGF (22, 29). We found that transforming growth factor-β_1, an important medi-

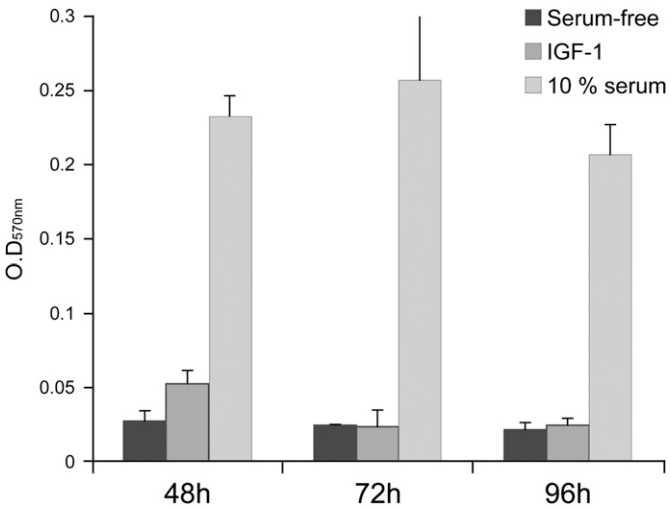

Figure 8. Fibroblast proliferation in response to insulin-like growth factor (IGF). Mouse lung fibroblasts were plated in triplicate and serum starved overnight followed by addition of IGF-I (100 ng/ml), serum-free medium (negative control), or 10% fetal bovine serum (FBS; positive control) and then incubated for the indicated times. Cell proliferation was measured by cell proliferation assay (MTT; Roche, Indianapolis, IN) assay. Data are shown as mean $OD_{570\ nm}$ and SD and represent the average of at least four independent experiments.

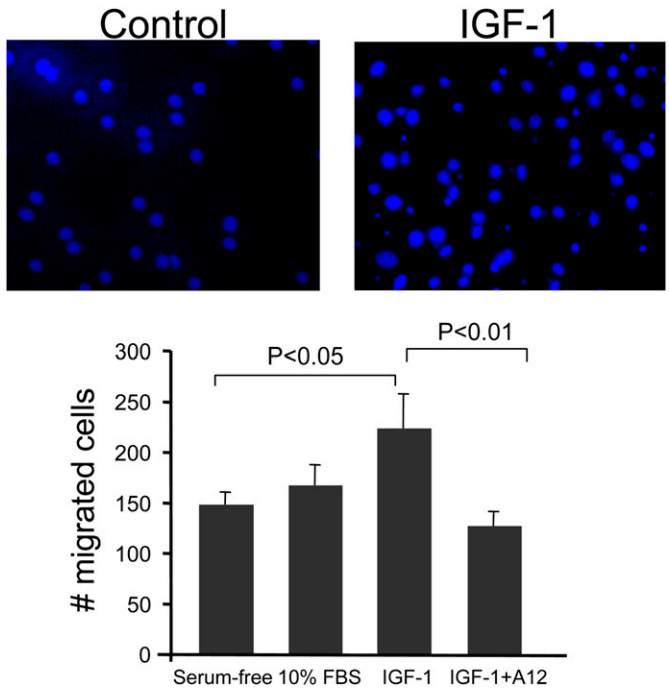

Figure 9. Insulin-like growth factor-I (IGF-I)–induced migration of fibroblasts. Mouse lung fibroblasts were plated on FluoroBlok transwell filters overnight, and then IGF-I (100 ng/ml), serum-free medium (negative control), or 10% serum (positive control) was added to the lower chamber. Some cells were preincubated with the blocking antibody to IGF-I receptor (A12, 40 μg/ml) before the addition of IGF-I. Cells were allowed to migrate through the membrane for 4 hours at 37°C. Migrated cells were counted by fluorescence microscopy. Each experiment was done in triplicate and repeated at least three times. Average cell counts and SD are presented.

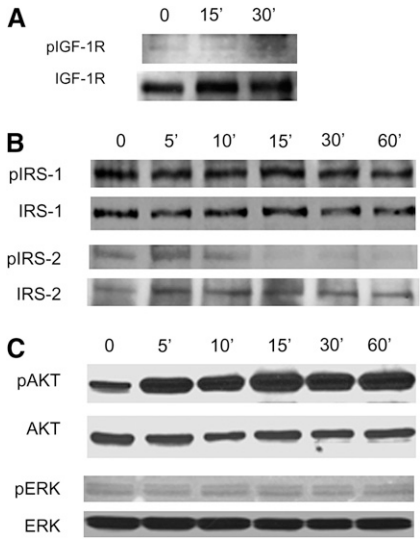

Figure 10. Mouse lung fibroblasts were serum starved overnight and then stimulated with insulin-like growth factor-I (100 ng/ml) for the indicated times. Cells were lysed, and proteins were separated by sodium dodecyl sulfate–polyacrylamide gel electrophoresis. Each membrane was blotted with the indicated phospho-antibody [(*A*) IGF-1R; (*B*) IRS-1, IRS-2 (*C*) AKT, ERK] and then stripped and reblotted with antibody to total protein.

ator of fibrosis, significantly up-regulated IGF-I expression in lung fibroblasts (data not shown).

We confirmed that lung fibroblasts express major components of the IGF signaling pathways including IGF-IR, IRS-1, and IRS-2. Interestingly, only IRS-2 showed increased phosphorylation after IGF-I stimulation. IRS-1 was present and phosphorylated at baseline and there was no change after IGF-I stimulation. Furthermore, Akt, but not ERK, was phosphorylated in response to IGF stimulation. The signaling response to IGF-I varies depending on the cell type examined (30). Both the PI3 kinase pathway and MAPK pathway are involved in IGF-IR–mediated signaling in carcinoma and other cell types (1). In myeloma cells, both antiapoptotic and proproliferative signaling from IGF-I was mediated by PI3 kinase (31). In myoblasts, IGF-I–induced differentiation was mediated by PI3 kinase, whereas proliferation was mediated by MAPK (20). In hepatocytes, IGF-mediated cell survival was dependent on IRS-2 (32). In our experiments, IGF-I stimulation selectively activated IRS-2 and the PI3 kinase pathway, and not IRS-1 and the MAPK pathway. Although IGF-I increases proliferation in many cell types (4, 18, 19, 26, 27, 31), we did not see any effect of IGF-I on lung fibroblast proliferation. Our results, however, are consistent with the selective activation of IRS-1 and IRS-2 leading to proliferation and migration, respectively, in pleural mesothelioma cells (18) and MCF cells (33).

One feature of pulmonary fibrosis is migration of fibroblasts into the intraalveolar space, where they secrete matrix proteins and contribute to the obliteration of normal architecture. We found that IGF-I induced migration of fibroblasts, which was inhibited by addition of A12. IGF-IR activation can affect cell migration through several mechanisms including down-regulation of adhesive strength of integrins (34), redistribution of integrins to the leading edge of migrating cells, and disruption of cadherin–catenin complexes (35). Because we previously detected elevated levels of IGF-I in BALF from patients with ARDS, IGF-I may provide a chemotactic factor for migration of fibroblasts into intraalveolar spaces, which results in deposition of matrix proteins and eradication of airspaces.

The mechanism of improved survival with early administration of A12 is not clear, but we speculate that the mechanism is distinct from an effect on improved fibrosis. There was no difference in hydroxyproline content on Days 7 and 14, suggesting that differences in early fibrosis did not account for the decreased mortality of A12-treated mice. Late administration of A12 did not affect survival. This is not surprising because the majority of deaths from bleomycin occur in the first 10 days after injury; it is unlikely that mice would be affected by late A12 administration. Suppression of the initial inflammatory response by A12 is possible. There was a trend toward decreased BALF cell counts and total protein in A12-treated mice, suggesting less inflammation, but this did not reach statistical significance. We did not see any differences in cell differentials at any time point. It is possible that earlier time points may have revealed differences in either lung permeability or inflammation that were subsequently reflected in mortality. A12 treatment may affect the response to oxidative stress after bleomycin injury. Consistent with this possibility, IGF-IR heterozygous mice are resistant to oxidative stress and have longer life spans, which may be due to decreased signaling through the p66 isoform of Shc, another signal transduction molecule for IGF-IR (36).

In summary, we show that early A12 administration improved survival of bleomycin-treated mice. In addition, although initial fibrosis was similar in control and A12-treated mice, A12-treated mice had faster resolution of fibrosis. Furthermore, late A12 administration also decreased fibrosis in bleomycin-treated mice. We speculate that some of the effects of A12 are due to increased fibroblast apoptosis, which facilitates matrix remodeling and resolution of fibrosis. These data show that the IGF-IR is a potential target for treatment of lung injury and fibrosis, and therapeutic reagents are already being developed and tested in patients.

***Conflict of Interest Statement*:** J.-E.C. does not have a financial relationship with a commercial entity that has an interest in the subject of this manuscript. S.-s.L. does not have a financial relationship with a commercial entity that has an interest in the subject of this manuscript. D.A.S. does not have a financial relationship with a commercial entity that has an interest in the subject of this manuscript. I.H. does not have a financial relationship with a commercial entity that has an interest in the subject of this manuscript. K.L.H. does not have a financial relationship with a commercial entity that has an interest in the subject of this manuscript. V.J.T. does not have a financial relationship with a commercial entity that has an interest in the subject of this manuscript. R.V. does not have a financial relationship with a commercial entity that has an interest in the subject of this manuscript. S.R.P. received $1,000 from ImClone for giving a talk on A12 at the JCO meeting in Orlando, Florida. L.M.S. has a patent application pending on "Compositions and Methods for the Treatment of Respiratory Disorders;" this patent application relates to methods for the treatment of respiratory disorders using inhibitors of IGF-IR activity or expression.

References

1. LeRoith D, Roberts CT Jr. The insulin-like growth factor system and cancer. *Cancer Lett* 2003;195:127–137.
2. Kurmasheva RT, Houghton PJ. IGF-I mediated survival pathways in normal and malignant cells. *Biochim Biophys Acta* 2006;1766:1–22.
3. Rom WN, Basset P, Fells GA, Nukiwa T, Trapnell BC, Crysal RG. Alveolar macrophages release an insulin-like growth factor I–type molecule. *J Clin Invest* 1988;82:1685–1693.
4. Maeda A, Hiyama K, Yamakido H, Ishioka S, Yamakido M. Increased expression of platelet-derived growth factor A and insulin-like growth factor-I in BAL cells during the development of bleomycin-induced pulmonary fibrosis in mice. *Chest* 1996;109:780–786.
5. Krein PM, Sabatini PJ, Tinmouth W, Green FH, Winston BW. Localization of insulin-like growth factor-I in lung tissues of patients with fibroproliferative acute respiratory distress syndrome. *Am J Respir Crit Care Med* 2003;167:83–90.
6. Schnapp LM, Donohoe S, Chen J, Sunde DA, Kelly PM, Ruzinski J, Martin T, Goodlett DR. Mining the acute respiratory distress syndrome proteome: identification of the insulin-like growth factor (IGF)/IGF-binding protein-3 pathway in acute lung injury. *Am J Pathol* 2006;169:86–95.

7. Iredale JP, Benyon RC, Pickering J, McCullen M, Northrop M, Pawley S, Hovell C, Arthur MJ. Mechanisms of spontaneous resolution of rat liver fibrosis: hepatic stellate cell apoptosis and reduced hepatic expression of metalloproteinase inhibitors. *J Clin Invest* 1998;102:538–549.
8. Phan SH. The myofibroblast in pulmonary fibrosis. *Chest* 2002;122:286S–289S.
9. Uhal BD. Apoptosis in lung fibrosis and repair. *Chest* 2002;122:293S–298S.
10. Cerwenka A, Morgan TM, Harmsen AG, Dutton RW. Migration kinetics and final destination of type 1 and type 2 CD8 effector cells predict protection against pulmonary virus infection. *J Exp Med* 1999; 189:423–434.
11. Burtrum D, Zhu Z, Lu D, Anderson DM, Prewett M, Pereira DS, Bassi R, Abdullah R, Hooper AT, Koo H, *et al.* A fully human monoclonal antibody to the insulin-like growth factor I receptor blocks ligand-dependent signaling and inhibits human tumor growth in vivo. *Cancer Res* 2003;63:8912–8921.
12. Wu JD, Odman A, Higgins LM, Haugk K, Vessella R, Ludwig DL, Plymate SR. *In vivo* effects of the human type I insulin-like growth factor receptor antibody A12 on androgen-dependent and androgen-independent xenograft human prostate tumors. *Clin Cancer Res* 2005; 11:3065–3074.
13. Matute-Bello G, Wurfel MM, Lee JS, Park DR, Frevert CW, Madtes DK, Shapiro SD, Martin TR. Essential role of MMP-12 in Fas-induced lung fibrosis. *Am J Respir Cell Mol Biol* 2007;37:210–221.
14. Ullman-Cullere MH, Foltz CJ. Body condition scoring: a rapid and accurate method for assessing health status in mice. *Lab Anim Sci* 1999;49:319–323.
15. Woessner JF Jr. The determination of hydroxyproline in tissue and protein samples containing small proportions of this imino acid. *Arch Biochem Biophys* 1961;93:440–447.
16. Ashcroft T, Simpson JM, Timbrell V. Simple method of estimating severity of pulmonary fibrosis on a numerical scale. *J Clin Pathol* 1988;41:467–470.
17. Qiang YW, Yao L, Tosato G, Rudikoff S. Insulin-like growth factor I induces migration and invasion of human multiple myeloma cells. *Blood* 2004;103:301–308.
18. Hoang CD, Zhang X, Scott PD, Guillaume TJ, Maddaus MA, Yee D, Kratzke RA. Selective activation of insulin receptor substrate-1 and -2 in pleural mesothelioma cells: association with distinct malignant phenotypes. *Cancer Res* 2004;64:7479–7485.
19. Coolican SA, Samuel DS, Ewton DZ, McWade FJ, Florini JR. The mitogenic and myogenic actions of insulin-like growth factors utilize distinct signaling pathways. *J Biol Chem* 1997;272:6653–6662.
20. Selman Lama M. Pulmonary fibrosis: human and experimental disease. In: Roskind M, editor. Connective tissue in health and disease. Boca Raton, FL: CRC Press; 1990. pp. 123–188.
21. Thannickal VJ, Toews GB, White ES, Lynch JP III, Martinez FJ. Mechanisms of pulmonary fibrosis. *Annu Rev Med* 2004;55:395–417.
22. Scarpa RC, Carraway RE, Cochrane DE. Insulin-like growth factor (IGF) induced proliferation of human lung fibroblasts is enhanced by neurotensin. *Peptides* 2005;26:2201–2210.
23. Goldstein RH, Poliks CF, Pilch PF, Smith BD, Fine A. Stimulation of collagen formation by insulin and insulin-like growth factor I in cultures of human lung fibroblasts. *Endocrinology* 1989;124:964–970.
24. Oldroyd SD, Miyamoto Y, Moir A, Johnson TS, El Nahas AM, Haylor JL. An IGF-I antagonist does not inhibit renal fibrosis in the rat following subtotal nephrectomy. *Am J Physiol Renal Physiol* 2006; 290:F695–F702.
25. Frankel SK, Moats-Staats BM, Cool CD, Wynes MW, Stiles AD, Riches DW. Human insulin-like growth factor-IA expression in transgenic mice promotes adenomatous hyperplasia but not pulmonary fibrosis. *Am J Physiol Lung Cell Mol Physiol* 2005;288:L805–L812.
26. Allen JT, Bloor CA, Knight RA, Spiteri MA. Expression of insulin-like growth factor binding proteins in bronchoalveolar lavage fluid of patients with pulmonary sarcoidosis. *Am J Respir Cell Mol Biol* 1998; 19:250–258.
27. Harrison NK, Cambrey AD, Myers AR, Southcott AM, Black CM, du Bois RM, Laurent GJ, McAnulty RJ. Insulin-like growth factor-I is partially responsible for fibroblast proliferation induced by bronchoalveolar lavage fluid from patients with systemic sclerosis. *Clin Sci (Lond)* 1994;86:141–148.
28. Mutsaers SE, Harrison NK, McAnulty RJ, Liao JY, Laurent GJ, Musk AW. Fibroblast mitogens in bronchoalveolar lavage (BAL) fluid from asbestos-exposed subjects with and without clinical evidence of asbestosis: no evidence for the role of PDGF, TNF-α, IGF-1, or IL-1β. *J Pathol* 1998;185:199–203.
29. Danielpour D, Song K. Cross-talk between IGF-I and TGF-β signaling pathways. *Cytokine Growth Factor Rev* 2006;17:59–74.
30. Petley T, Graff K, Jiang W, Yang H, Florini J. Variation among cell types in the signaling pathways by which IGF-I stimulates specific cellular responses. *Horm Metab Res* 1999;31:70–76.
31. Qiang YW, Kopantzev E, Rudikoff S. Insulinlike growth factor-I signaling in multiple myeloma: downstream elements, functional correlates, and pathway cross-talk. *Blood* 2002;99:4138–4146.
32. Valverde AM, Fabregat I, Burks DJ, White MF, Benito M. IRS-2 mediates the antiapoptotic effect of insulin in neonatal hepatocytes. *Hepatology* 2004;40:1285–1294.
33. Zhang X, Kamaraju S, Hakuno F, Kabuta T, Takahashi S, Sachdev D, Yee D. Motility response to insulin-like growth factor-I (IGF-I) in MCF-7 cells is associated with IRS-2 activation and integrin expression. *Breast Cancer Res Treat* 2004;83:161–170.
34. Lynch L, Vodyanik PI, Boettiger D, Guvakova MA. Insulin-like growth factor I controls adhesion strength mediated by $\alpha_5\beta_1$ integrins in motile carcinoma cells. *Mol Biol Cell* 2005;16:51–63.
35. Andre F, Rigot V, Thimonier J, Montixi C, Parat F, Pommier G, Marvaldi J, Luis J. Integrins and E-cadherin cooperate with IGF-I to induce migration of epithelial colonic cells. *Int J Cancer* 1999;83:497–505.
36. Holzenberger M, Dupont J, Ducos B, Leneuve P, Geloen A, Even PC, Cervera P, Le Bouc Y. IGF-1 receptor regulates lifespan and resistance to oxidative stress in mice. *Nature* 2003;421:182–187.